Petroleum Science and Engineering
2024; 8(1): 7-15
http://www.sciencepublishinggroup.com/j/pse
doi: 10.11648/j.pse.20240801.12
ISSN: 2640-4486 (Print); ISSN: 2640-4516 (Online)

Two-dimensional Numerical Analysis of Waves at Interface of Laminar Core-annular Flow in Vertical Pipe: Detailed Investigation of Influence of Several Physical Parameters

Gijsbert Ooms*, Mathieu Pourquie

J. M. Burgerscentrum, Mechanical Engineering, Delft University of Technology, Delft, The Netherlands

Email address:
prof.ooms@gmail.com (Gijsbert Ooms)
*Corresponding author

To cite this article:
Gijsbert Ooms, Mathieu Pourquie. (2024). Two-dimensional Numerical Analysis of Waves at Interface of Laminar Core-annular Flow in Vertical Pipe: Detailed Investigation of Influence of Several Physical Parameters. *Petroleum Science and Engineering, 8*(1), 7-15.
https://doi.org/10.11648/j.pse.20240801.12

Received: December 22, 2023; **Accepted:** January 3, 2024; **Published:** January 24, 2024

Abstract: In this study, a two-dimensional numerical analysis is made of the waves at the interface between the core and the annulus of a laminar core-annular flow in a vertical pipe. The Reynolds number did not exceed 600. The volume-of-fluid method in the interFoam solver from the OpenFOAM software package (version 2.1) was used. This solver employs finite volume discretization, and cell face interpolated variables play a major role in the solution algorithm. The influences on the waves of the pressure drop along the pipe, the buoyancy due to the density difference between the core liquid and annular liquid, the thickness of the annular layer, the viscosity of the core liquid, and the pipe length were considered. The surface tension at the interface in relation to several of these factors was also considered. In addition, theoretical and experimental results of previous studies were compared with our numerical results. Novel results were obtained that indicated the effects of the surface tension, pipe length, and thickness of the annular layer on the waves in laminar core-annular flow. Possible fouling of the pipe wall by the core liquid was also considered. The study and practical application of core-annular flow were found to be possible using numerical analysis.

Keywords: Waves, Laminar Core-annular Flow, Vertical Pipe, Numerical Study

1. Introduction

Core-annular flow is the flow of a high-viscosity liquid core surrounded by a low-viscosity liquid.

It has been used for the transport of heavy oil in a vertical or horizontal pipe to significantly reduce the pressure drop over the pipe. The historical development of core-annular flow was outlined by Joseph et al. [1].

The behavior of waves at the interface of a laminar core-annular flow through a vertical pipe has received considerable research attention (e.g., Bai et al. [2], Ghosh et al. [3], Chen et al. [4], Rodriguez and Bannwart [5], Brauner and Maron [6], and Rodriguez and Bannwart [7]). Starting with a flat interface, a small wave can emerge that increases in amplitude and possibly changes its shape. After some time, the wave becomes constant in amplitude and shape and travels with a certain velocity at the interface. However, it is also possible that the wave does not become constant and instead becomes unstable. Small droplets of the core liquid are drawn from the interface into the annular layer, which can foul the pipe wall. The wave can continue to grow until it contacts and fouls the pipe wall. The conditions under which this phenomenon occurs depends on the physical properties of the flow, such as the surface tension at the interface, pressure drop over the pipe, buoyancy due to the density difference between the core liquid and annular liquid, and viscosity ratio of the two liquids. Moreover, the thickness of the annular layer influences the wave behavior. Beerens et al. [8] developed a two-dimensional numerical model of the laminar vertical core-annular flow in a pipe. Their numerical results were compared with theoretical results obtained from linear stability calculations and experimental data. They found that it is

possible to simulate core-annular flow through a pipe using the volume-of-fluid method.

In this study, the influences on the waves at the interface of laminar core-annular flow as a function of several physical parameters were investigated in detail. Novel results were obtaiined that indicated the effects of the surface tension, pipe length, and thickness of the annular layer on the waves in laminar core-annular flow.

2. Numerical Solution Method

The volume-of-fluid method in the interFoam solver from the OpenFOAM (Open Field Operation and Manipulation) software package (version 2.1) was ued. This solver employs finite volume discretization, and cell face interpolated variables play a major role in the solution algorithm. Because the viscosity and density in the laminar core-annular flow are nonuniform, an indicator function was used, which was transported through the domain using an advection equation. This equation was solved in conjunction with the Navier-Stokes and mass conservation equations. Despande et al. [9] described how this is achieved. These equations were solved using a fixed grid. The grids were equidistant, orthogonal, and nonstretched. Grid points of (64 64), (128 128), and (256 256) were used. Grid sensitivity tests were performed to select the best grid considering accuracy and practicality. The interFoam solver used an adjustable timestep based on the maximum Courant number in the domain. In addition to the Courant number, several other physical timescales had a significant influence on the stability and accuracy of the solver. For instance, the surface tension imposed a restriction on the timestep. The following discretization schemes were applied: backward Euler in time, limited linearity for the advection terms of the velocity components, and the van Leer scheme for the advection of the scalar components. Pressure–velocity coupling was performed using the PIMPLE scheme. A preconditioned conjugate gradient for the pressure and preconditioned biconjugate gradient for the velocity components were used as linear solvers. A no-slip condition was applied to the pipe wall. At the pipe inflow and outflow cross sections, a periodic boundary condition was applied, implying that the length of the calculation domain was equal to an integer number of wavelengths at the core-annular interface. The initial velocity distribution was chosen to be equal to the analytical solution of the Navier–Stokes equation for a core-annular flow with a smooth interface. The initial interfacial surface was disturbed by a sine wave with a small amplitude.

3. Results

3.1. Influences of Δp, g, and σ

A first investigation was made of a case (Case 1) with the following properties:

Pipe length (l) = 0.0116 m;

Pressure drop (Δp) = 0 kg/m^2s^2;

Surface tension (σ) = 0 kg/s^2;

Gravity constant (g) = 0 m/s^2;

Kinematic viscosity of the annular liquid (ν_w) = 0.000001 m^2/s;

Dynamic viscosity of the annular liquid (μ_w) = 0.000995 kg/ms;

Kinematic viscosity of the core liquid (ν_o) = 0.000663 m^2/s;

Dynamic viscosity of the core liquid (μ_o) = 0.6 kg/ms;

Density of the annular liquid (ρ_w) = 995 kg/m^3;

Density of the core liquid (ρ_o) = 905 kg/m^3;

Pipe radius (R_2) = 0.0047554 m;

Core radius (R_1) = 0.0037192 m;

Starting wave amplitude at the interface = 0.000001 m;

Starting velocity of the liquid in the annular and core layers (U_z) = 0 m/s;

Velocity of the pipe wall = -0.166 m/s;

Starting time = 0 s.

The calculation results for this case are shown as Case 1 in Figure 1.

Because Δp = 0 kg/m^2s^2, g = 0 m/s^2, and σ = 0 kg/s^2, all the forces are zero, and there is no wave development at the interface.

In Case 2 shown in Figure 1, a finite pressure force was incorporated.

Δp = 9303 kg/m^2s^2.

Five waves with small amplitudes developed as a function of time and remained constant in shape, moving at a certain velocity at the interface. Owing to the pressure force, the high-viscosity core generated a shear force at the interface with the low-viscosity annulus to generate waves. Because there was no surface tension, the interface tended to become unstable as small chunks of the core liquid were drawn into the annular layer. Using an extremely small timestep of $\mathcal{O}(10^{-7})$, it was possible to maintain the wave stability.

In Case 3 (Figure 1), another force was added: the acceleration due to gravity (g = -9.81 m/s^2). Only one wave developed at the interface. When the amplitude was large, the wave almost contacted the pipe wall and finally moved with a constant velocity along the interface. The wave never fouled the pipe wall, because the pressure and viscous forces kept it free from the wall. Owing to the density difference between the core and annulus, the gravitational force generated a buoyancy force, causing an additional contribution to the shear force at the interface. Therefore, the wave remained more stable, and a larger timestep of $\mathcal{O}(10^{-5})$ was sufficient in this case.

In Case 4 (Figure 1), the surface tension of the interface (σ = 0.0170 kg/s^2) was considered. This property tends to dampen the wave, as can be observed by comparing Cases 3 and 4. The amplitude of the wave decreased with an increase in the surface tension. When the surface tension increases, the wave is reduced to a flat surface.

The mesh dependence for Case 3, as shown in Figure 1 was also studied by conducting calculations with a mesh of (128 0 128) and a mesh of (256 0 256). The results are shown

as Case 5 in Figure 2. There is no significant difference between these two figures, indicating that the chosen mesh size of (128 0 128) is sufficient.

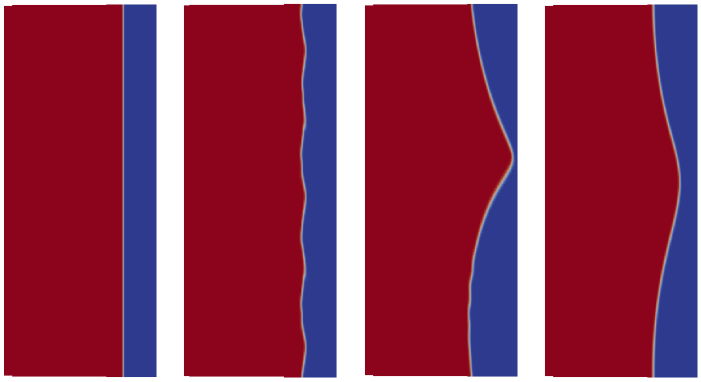

Figure 1. *Numerical results considering the effects of the pressure drop, gravity, and surface tension. First figure: Case 1; Second figure: Case 2; Third figure: Case 3; Fourth figure: Case 4.*

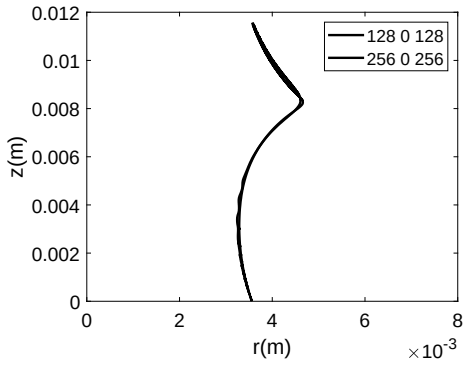

Figure 2. *Case 5: Δp = 9303 kg/m^2s^2; g = -9.81; m/s^2; σ = 0 kg/s^2.*

3.2. Influence of the Thickness of the Annular Layer R_1

A study was made of the influence of the annular layer thickness on the waves at the interface. For the first case (Case 6), the same data as in Case 3 (Figure 1) was used with one exception the core radius R_1 = 0.0037192 m was decreased to R_1 = 0.0031 m. The calculation results for this case are shown as Case 6 in Figure 3. The broader annular layer significantly influenced the waves. The amplitude increased, and the wave shape changed considerably compared with the wave in Case 3 of Figure 1. In addition, small chunks of the core liquid were drawn from the interface into the annular layer and fouled the pipe walls. A further investigation of this case was made of the damping effect resulting from the surface tension at the interface and ,therefore, the surface tension was assumed to have a value of σ = 0.0170 kg/s^2. The results are shown as Case 7 in Figure 3. The effect of the surface tension was significant, as was observed by comparing Cases 6 and 7. A smooth wave developed without fouling due to the core liquid chunks in the annular layer.

For the next case (Case 8), the same data employed for Case 3 (Figure 1) was used with one exception: the core radius R_1 = 0.0037192 m was increased to 0.0040 m. The calculation results for this case are shown as Case 8 in Figure 3. Two waves developed, and their tops did not contact the pipe wall. However, small chunks of the core liquid were occasionally drawn from the interface into the annular layer, fouling the pipe wall.

Finally, the damping effect of Case 8 due to the surface tension was investigated. A surface tension at the interface with a value of σ = 0.0170 kg/s^2 was applied. The results are shown as Case 9 in Figure 3. Only one smooth wave was observed, with no fouling resulting from chunks of the core liquid in the annular layer. Therefore, as was observed previously, the influence of surface tension at the interface was considerable.

3.3. Influence of Viscosity of Core Liquid (ν_o)

In the previous calculations, the kinematic viscosity of the core liquid (ν_o = 0.000663 m^2/s) was assumed to be significantly higher than that of the annular layer (ν_w = 0.000001 m^2/s). The aim here was to investigate how long core-annular flow continues to exist for smaller values of ν_o. Case 4 (Figure 1) was selected as a reference for the initial conditions of this system and the viscosity was varied from ν_o = 0.000663 m^2/s to 0.000500 m^2/s. A flat interface was chosen for the initial calculation. The calculation result for this system is shown as Case 10 in Figure 4. Cases 4 (Figure 1) and 10 (Figure 4) were compared, and minimal variation was observed as the viscosity decreased from ν_o = 0.000663 m^2/s to 0.000500 m^2/s.

Therefore, the viscosity was furher reduced from ν_o = 0.000500 m^2/s to 0.000300 m^2/s in Case 11. A flat interface was again chosen for our initial calculation. The results for this case, as shown in Figure 4, were surprising, as the interface remained flat. This result was likely obtained because the lower viscosity of the core liquid resulted in the surface tension having a stronger grip on the interface, such that the interface was more easily flattened.

The calculation for Case 11 (Figure 4) was also performed using an initial finite amplitude and the same reduced viscosity

of ν_o = 0.000300 m^2/s; again, a flat interface was observed. To validate this assumption, the surface tension was reduced from σ = 0.0170 kg/s^2 to σ = 0.0085 kg/s^2. The results of this new case (Case 12) are shown in Figure 4. A wave was generated with a finite amplitude. The surface tension was also further reduced to σ = 0.0 kg/s^2 (Case 13); the results are shown in Figure 4. Because of the absence of surface tension, there was no damping effect on the wave. Small chunks of the core liquid were drawn from the tops of the wave into the annular layer and fouled the pipe wall in this case.

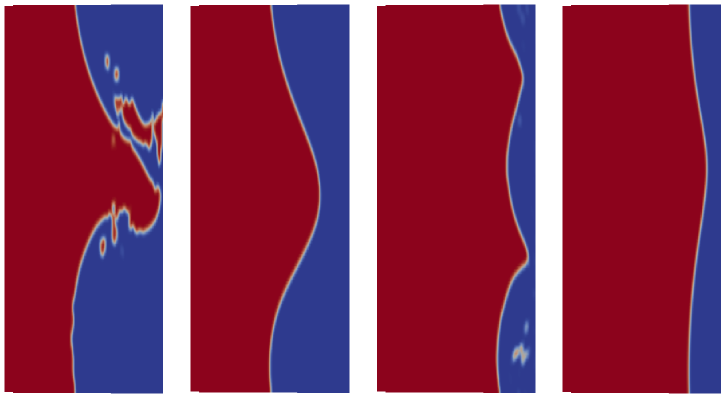

Figure 3. *Numerical results for the influence of the annular layer thickness. First figure: Case 6; Second figure: Case 7; Third figure: Case 8; Fourth figure: Case 9.*

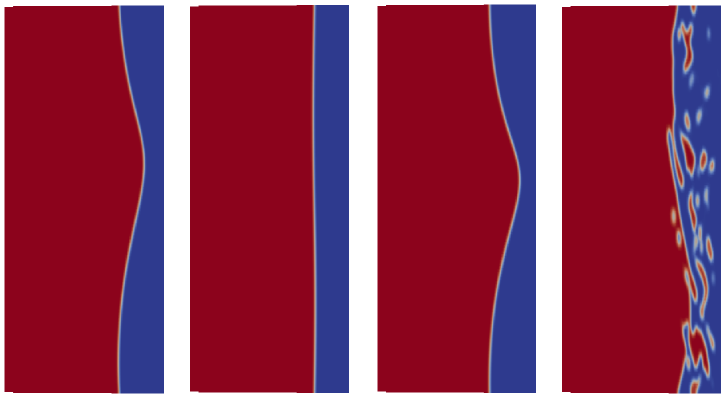

Figure 4. *Numerical results indicating the influence of the core liquid viscosity. First figure: Case 10; Second figure: Case 11; Third figure: Case 12; Fourth figure: Case 13.*

3.4. Influence of the Pipe Length (l)

By performing calculations for increasing pipe lengths, the length of the interfacial wave in a long pipe can be approximated. In Case 4 (Figure 1), a calculation was performed for a pipe with a length of $0.0116\ m$ and identified one wave. Therefore, a wavelength of $0.0116\ m$ was obtained in this case.

For the next calculation, a pipe length of $0.0232\ m$ was assumed (twice the length of the first pipe). The calculation began with two freely chosen waves at the interface (see Case 14-a in Figure 5). The calculation results are shown as Case 14-b in Figure 5. Two waves were observed; therefore, the wavelength was the same as that in Case 4 (Figure 1), i.e., l = $0.0116\ m$. For the next calculation, a pipe length of $0.0464\ m$ was used (four times the length of the first pipe. The start was again with four freely selected waves at the interface (see Case 15-a in Figure 5) and began the calculation. Subsequently, the amplitudes decreased until the interface became completely flat. Thereafter, the amplitudes began to increase, but only two waves were identified instead of four (see Case 15-b in Figure 5).

Therefore, a wavelength of $0.0232\ m$ was obtained in this case.

Next an investigation was made of the number of waves that are present when an increased pipe length of $0.0928\ m$ (eight times the length of the first pipe) is used. A statrt was made with eight freely selected waves at the interface (see Cases 16-a and 16-b in Figure 6) and started the calculations. Subsequently, the amplitudes of these waves decreased until the interface became completely flat. Thereafter, the amplitude started to increase again, but this time with four waves instead of eight (see Cases 16-c and 16-d in Figure 6). Therefore, the wavelength was 0.0232 in this case. For proper visualization, the domain in Figure (6) was divided into two components indicating the start of the calculation (left) and two components indicating the end of the calculation (right).

In the next calculation, a start was made with 16 freely

selected waves at the interface (see Cases 17-a and 17-b in Figure 7). As before, their amplitudes decreased until the interface became completely flat. Thereafter, the amplitude started to increase again but this time with waves of different wavelengths (see Cases 17-c and 17-d in Figure 7. The wavelengths were 0.0441, 0.0285, 0.0202, 0.0191, 0.0272, 0.0132, and 0.0333 m. Therefore, the number of waves decreased from 16 to 7, and the wavelengths increased.

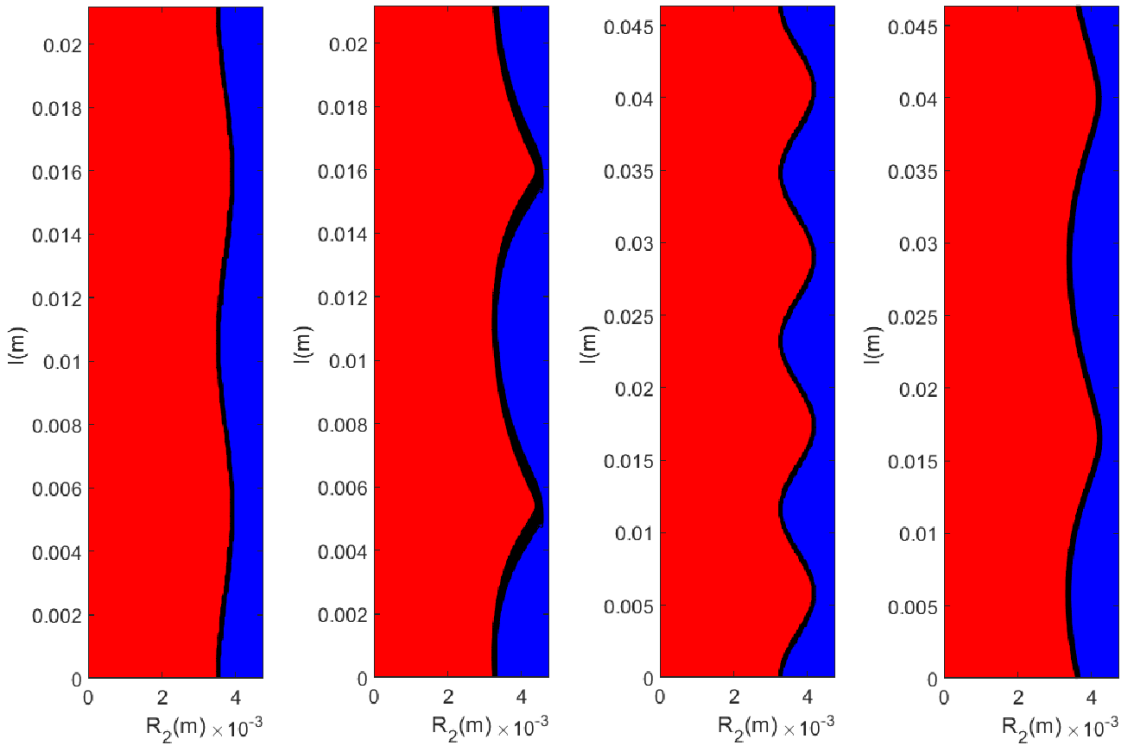

Figure 5. *Numerical results indicating the effect of the pipe length. First figure: Case 14-a; second figure: Case 14-b; third figure: Case 15-a; fourth figure: Case 15-b.*

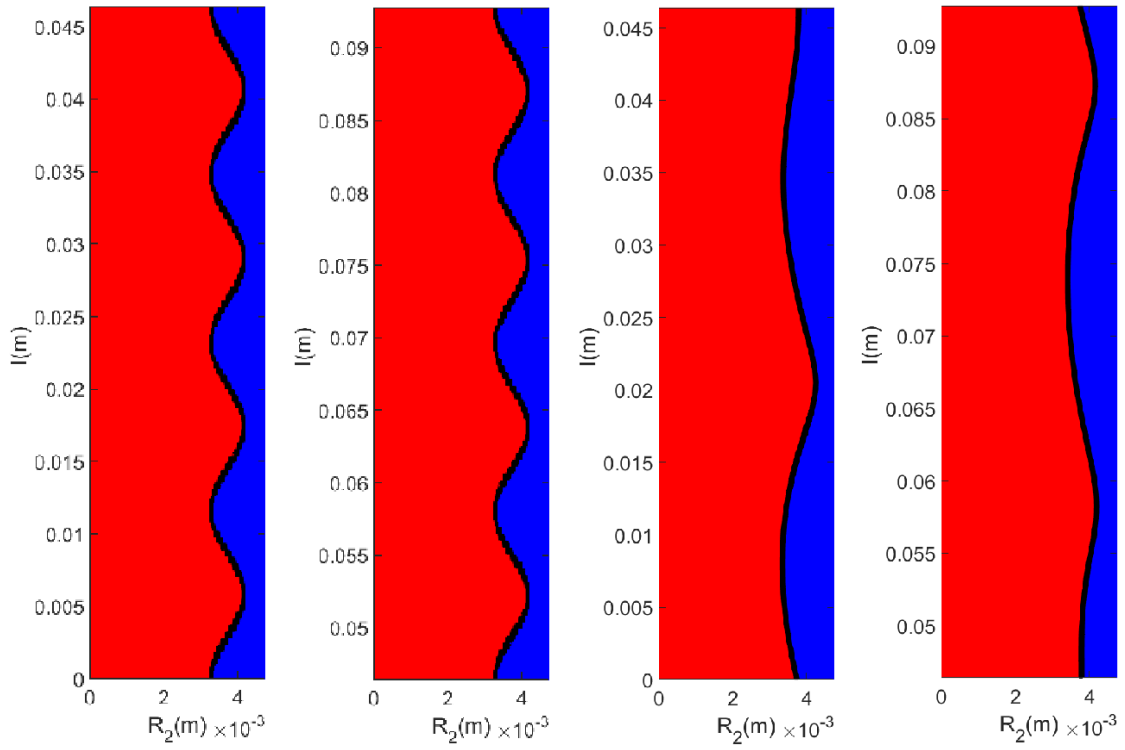

Figure 6. *Numerical results indicating the effect of the pipe length. First figure: Case 16-a; second figure: Case 16-b; third figure: Case 16-c; fourth figure: Case 16-d. For proper visualization, the domain is divided in two pieces for the start of the calculation (left) and two pieces for the end of the calculation (right).*

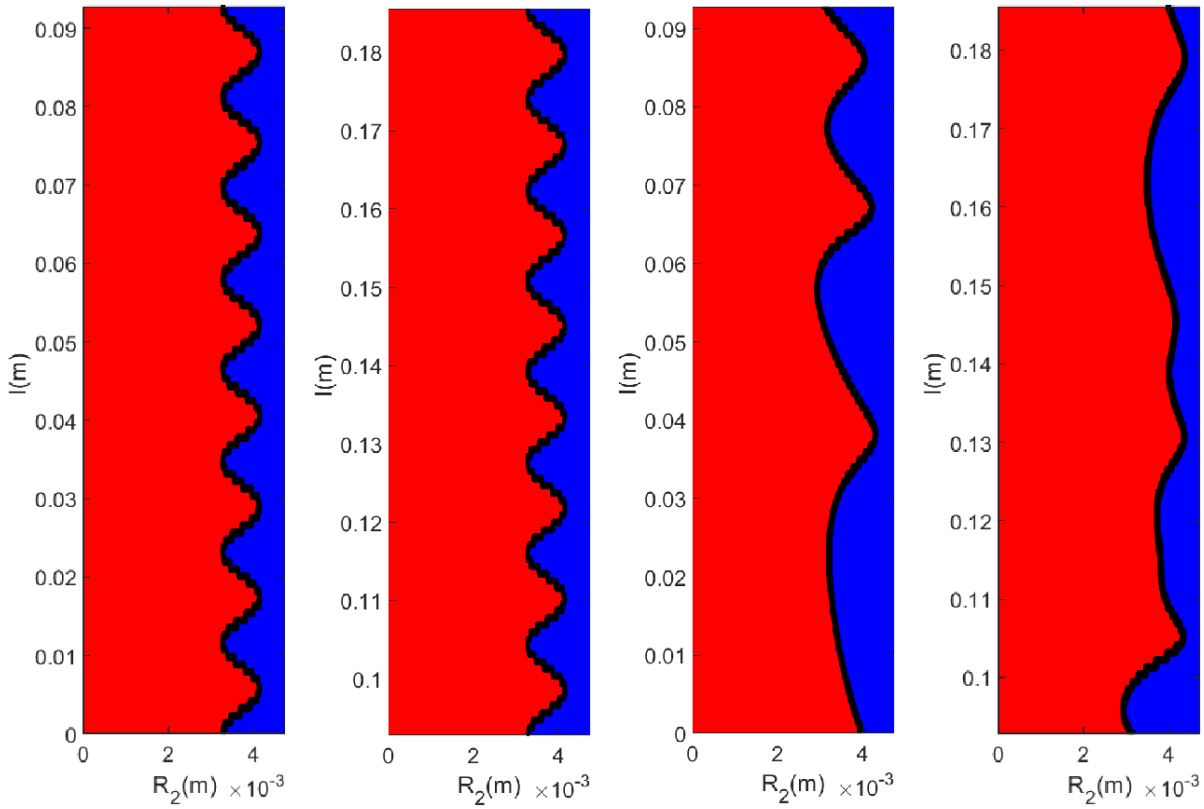

Figure 7. *Numerical results indicating the effect of the pipe length. First figure: Case 17-a; second figure: Case 17-b; third figure: Case 17-c; fourth figure: Case 17-d. For proper visualization, the domain is divided in two pieces for the start of the calculation (left) and two pieces for the end of the calculation (right).*

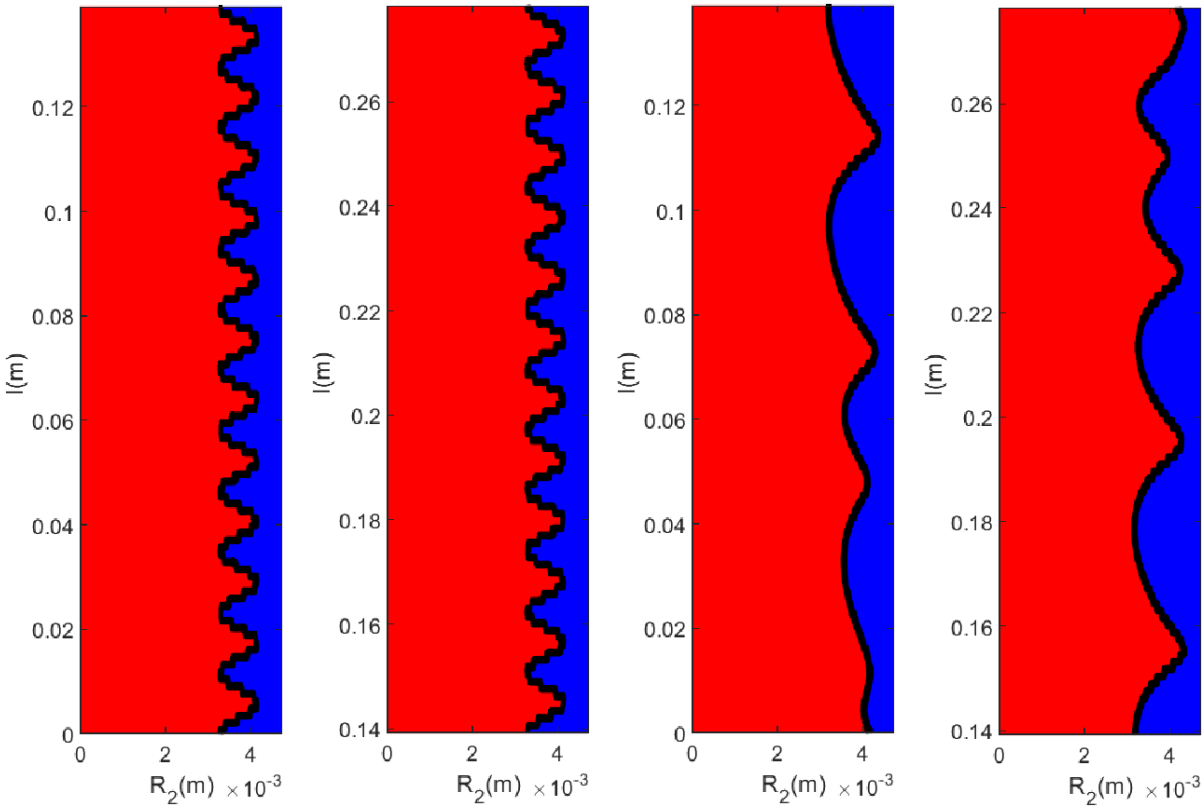

Figure 8. *Numerical results indicating the effect of the pipe length. First figure: Case 18-a; second figure: Case 18-b; third figure: Case 18-c; fourth figure: Case 18-d. For proper visualization, the domain is divided in two pieces for the start of the calculation (left) and two pieces for the end of the calculation (right).*

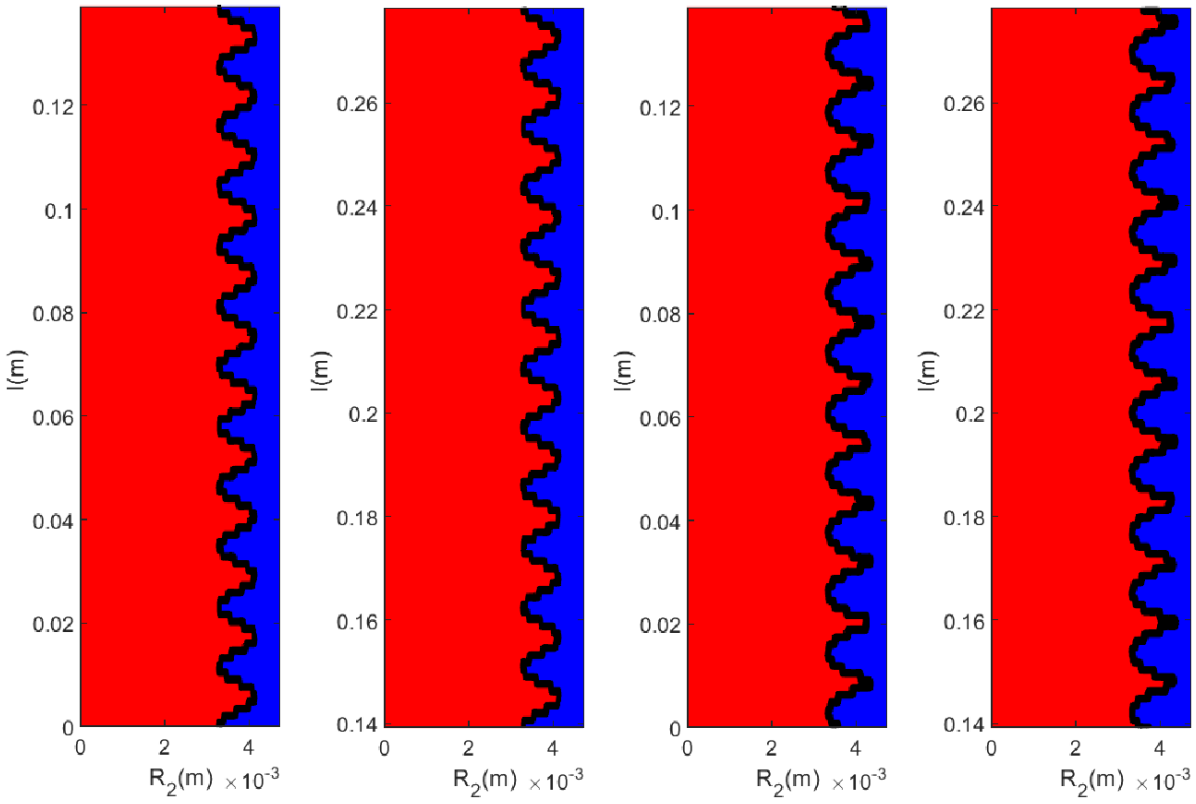

Figure 9. *Numerical results indicating the effect of the pipe length. First figure: Case 19-a; second figure: Case 19-b; third figure: Case 19-c; fourth figure: Case 19-d. For proper visualization, the domain is divided in two pieces for the start of the calculation (left) and two pieces for the end of the calculation (right).*

Next, a start was made with 24 freely chosen waves at the interface (see Cases 18-a and 18-b in Figure 8). The amplitudes decreased until the interface became completely flat. Thereafter, the amplitude started to increase again with waves of different wavelengths (see Cases 18-c and 18-d in Figure 8). The wavelengths were 0.0178, 0.0357, 0.0232, 0.0428, 0.0418, 0.0393, 0.0321, 0.0250, and 0.0214 m. Therefore, the number of waves decreased from 16 to 9, and the wavelengths increased.

This last calculation was repeated with a smaller value of surface tension, reducing it from (σ) = 0.0850 kg/s^2 to 0.0085 kg/s^2 (see Cases 19-a and 19-b in Figure 9 for the start of the calculation and Cases 19-c and 19-d for the end of the calculation). The effect of the smaller surface tension value was considerable. The number of waves remained constant as a function of time; therefore, the wavelength was 0.0116 m.

3.5. Comparison with Theory

Next a comparison was made between our numerical calculation results and theoretical predictions considering the results of [10], in which linear stability theory was investigated in the case of free-fall conditions under the influence of gravity. The graphical results of that study indicated several regions where, according to the linear stability theory, the core-annular flow is either stable or unstable. The numerical method usrd in this study (based on the Navier–Stokes equation) was applied to several points in this graph to compare the results with those of linear stability theory. It should be noted that a comparison between numerical calculation results based on the Navier–Stokes equation and linear stability theory has also been performed by Li and Renardi [11] and Beerens et al. [8]). A start was made with a stable case described by the following dimensionless groups:

$a = R_2/R_!$=1.1
$m = \mu_2/\mu_2 = 0.5$
$\Delta p = 0$
$J = \sigma R_2/\rho_1 \nu_!{}^2 = 2000$
$\zeta = \rho_!/\rho_@ = 1.4$
$R_g = R_!(gR_!))^{1/2}/\nu_! = 30.$
Here, R_g represents the Reynolds number based on gravity
$\lambda = l/R_1 = 0.0116/0.00432 = 2.685$
$\alpha = 2\pi/\lambda = 2.340.$

The case was allowed to operate over a long period. The results are shown as Cases 20-a (start of the calculation) and 20-b (end of the calculation) in Figure 10. The interface remained flat; therefore, the flow was stable.

Next,the same case conditions were selected but with an initial wavy interface (see Case 21-a in Figure 11) and started the calculation. The results again exhibited a flat interface, indicating that the flow was stable (see Case 21-b in Figure 11).

Subsequently, an unstable case of free fall under gravity was selected, which is described by the following dimensionless groups: $a = R_2/R_!$=1.1
$m = \mu_2/\mu_2 = 0.5$
$\Delta p = 0$

$J = \sigma R_2/\rho_1 \nu_!{}^2 = 2000$
$\zeta = \rho_!/\rho_@ = 1$
$R_g = R_!(gR_!))^{1/2}/\nu_! = 5$
$\lambda = l/R_1 = 0.0116/0.000923 = 4\pi$
$\alpha = 2\pi/\lambda = 0.5$.

The results are shown in Cases 22-a (start of the calculation) and 22-b (end of the calculation) in Figure 12. The flow was found to be unstable. The interface developed from a smooth layer to an interface with three waves.

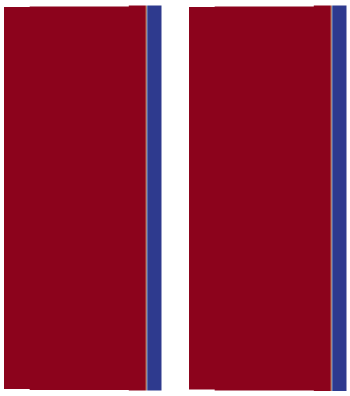

Figure 10. *Comparison with theory. Stable free fall case. Flat initial interface. Left: Case 20-a; right: Case 209-b.*

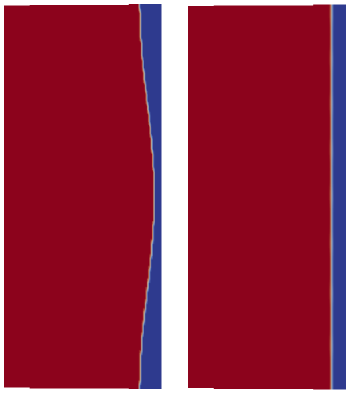

Figure 11. *Comparison with theory. Stable free fall case. Wavy initial interface. Left: Case 21-a; right: Case 21-b.*

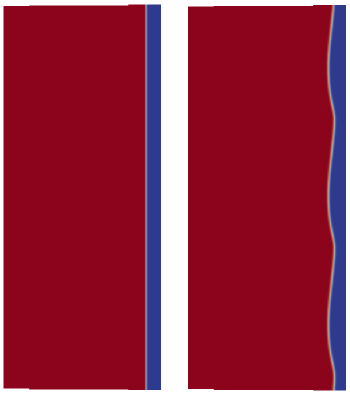

Figure 12. *Comparison with theory. Unstable free fall case. Flat initial interface. Left: Case 22-a; right: Case 22-b.*

Next, an investigation was made of the results of linear stability theory when applied to a case of forced flows, where a pressure drop is considered in addition to gravity. The referenced graph for this case in [10] (on p. 147) shows several regions where, according to the linear stability theory, the core-annular flow is either stable or unstable.

The numerical method of this study was applied to an unstable point in this graph to compare the results with those of linear stability theory. This point also relates to the experiment shown in [10] (on p. 123). The results are shown in Cases 23-a (start of the calculation) and 23-b (end of the calculation) in Figure 13. The flow was found to be unstable. The interface developed from a smooth layer to a spherical droplet of the core liquid. The formation of this droplet is a consequence of capillary instability resulting from the surface tension between the two liquids. Additionally, this droplet was observed in the experiment documented in [10] (on p. 123).

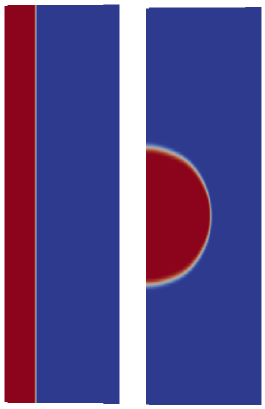

Figure 13. *Comparison with theory. Unstable forced flow case. Flat initial interface. Left: Case 23-a; right: Case 23-b.*

4. Conclusion

The calculations of this study indicated the strong effect of surface tension (see Cases 4, 5, 6, 7, 11, 12, 18-c, and 18-d). In particular, the effect of the surface tension on the wavelength of a long pipe was observed. In addition, the influence of the thickness of the annular layer and the viscosity of the core liquid are important parameters influencing the behavior of core-annular flow. Experiments in which the surface tension and viscosity of the core liquid can be varied should be investigated in future studies.

5. Discussion

Many parameters influence the behavior of core-annular flow, including the viscosities and densities of the core and annular liquids, length and width of the pipe, pressure drop over the pipe, surface tension at the interface between the two fluids, thickness of the annular layer, and presence of gravity. Even if these parameters are formulated using dimensionless groups, the number of combinations of these

groups is considerably large, and it is difficult to investigate their effects.

Therefore, in this study, a limited number of parameters was investigated. It was found to be possible to numerically investigate the behavior of core-annular flow. The results of the numerical calculations agreed well with theoretical and experimental results obtained from the literature.

In a future study, it is the intention to conduct a three-dimensional numerical analysis of the waves at the interface of a laminar core-annular flow in a horizontal pipe. In such conditions, the core eccentricity in the pipe, which is attributed to the density difference between the core and annular liquids, plays an important role.

The turbulent core-annular flow in a vertical or horizontal pipe has been studied, for instance, by Li et al. [12], Ingen Housz et al. [13] and Kim and Choi [14]. A study of fouling was carried out by Fan er al. [15].

Abbreviations

OpenFOAM: Open Field Operation and Manipulation

Conflicts of Interest

The authors declare no conflicts of interest.

References

[1] D. D. Joseph, R. Bai, K. R. Chen, and Y. Y. Renardy, Core-annular flows. Annu. Rev. Fluid Mech. 29, 65-40, 1997.

[2] R. Bai, K. Kelkar, and D. D. Joseph, Direct simulation of interfacial waves in a high-viscosity ratio, axisymmetric core-annular flow. J. Fluid Mech. 327, 1-34, 1996.

[3] S. Ghosh, G. Das, and P. K. Das, Simulation of core annular downflow through CFD ¨C A comprehensive study. Chem. Eng. Process. 49, 1222-1228, 2010.

[4] K. Chen, R. Bai, and D. D. Joseph, Lubricated pipelining. Part 3: Stability of core-annular flow in vertical pipes. J. Fluid Mech. 214, 251-286, 1990.

[5] O. M. Rodriguez and A. C. Bannwart, Experimental study of interfacial waves in vertical core flow. J. Petroleum Sci. Eng. 54, 140-148, 2006.

[6] N. Brauner and D. M. Maron, Classification of liquid-liquid two-phase flow systems and the prediction of flow pattern maps. 2nd Int. Symp. Two-Phase Flow Modeling and Experimentation, vol. 99, pp. 747-754, 1995.

[7] O. M. Rodriguez and A. C. Bannwart, Analytical model for interfacial waves in vertical core flow. J. Petroleum Sci. Eng. 54, 173-182, 2006.

[8] J. C. Beerens, G. Ooms, M. J. B. M. Pourquie, and J. Westerweel, A comparison between numerical predictions and theoretical and experimental results for laminar core-annular flow. AIChE J. 60, 3046-3056, 2014.

[9] S. Deshpande, L. Ammolu, and M. Trujillo, Evaluating the performance of the two-phase flow solver interFoam. Comput. Sci. Discovery 5, 014016, 2012.

[10] D. D. Joseph and Y. Y. Renardy, Fundamentals of Two Fluid Dynamics, Part II: Lubricated Transport, Springer Science+Business Media, New York, 1993.

[11] J. Li and Y. Renardi, Direct simulation of unsteady axisymmetric core-annular flow with high viscosity ratio. J. Fluid Mech. 391, 123-149, 1999.

[12] H. Li, M. J. B. M. Pourquie, G. Ooms, and R. A. W. M. Henkes, Simulation of turbulent annulus with interfacial waves in core-annular pipe flow. Int. J. Multiph. Flow 154, 104152, 2022.

[13] E. Ingen Housz, G. Ooms, R.A.W.M. Henked and M. J. B. M. Pourquie, A comparison between numerical predictions and experimental results for horizontal core-annular flow with a turbulent annulus. Int. J. Multiph. Flow 95, 271-282, 2017.

[14] K. Kim and H. Choi, Direct numerical simulation of a turbulent core-annular flow with water-lubricated high viscosity oil in a vertical pipe. J. Fluid Mech. 849, 419-447, 2018.

[15] J. Fan, H. Li, M. J .B. M. Pourquie, G. Ooms and R. A. W. M. Henkes, Simulation of the hydrodynamics in the onset of fouling for oil-water core-annular flow in a horizontal pipe. J. Petroleum Sci. Eng. 207, 109084, 2021.